Theoretical and Computational Studies in Intermediate Energy Nuclear Physics

Final Report for Period

November 1, 1992 - October 31, 1995

Charlotte Elster

Asst. Professor
Institute of Nuclear and Particle Physics
Department of Physics and Astronomy
Ohio University
Athens, OH 45701

April 1995

Prepared for:

The United States Department of Energy

Grant No. DE-FG02-93ER40756

PROGRESS REPORT, APRIL 1994

During the first two and one half years of the current grant from the U.S. Department of Energy significant progress was made in the applications of many-body scattering theory to nuclear systems and studies of few-body systems described by effective hadronic field theories. The report is structured correspondingly into to sections describing the progress and achievements in each subarea.

1. Application of Many-Body Scattering Theory to Nuclear Systems.

A long-standing aim of 'classical' nuclear physics has been the application of the nuclear force as obtained from two-nucleon data and the prediction of many-body phenomena therefrom. During the last two and one half years of the current grant from the U.S. Department of Energy, the PI and collaborators have made considerable progress towards this goal in the area of nucleon scattering from nuclei at intermediate energies. This progress has partially been due to the rapid developments in high performance computing technologies.

The following subsections describe in some detail the work carried out under the the current grant from the U.S. Department of Energy, which is a first time award for the PI.

(a) Modification of the Scattering Process due to the Presence of the Nuclear Medium.

This part of the work performed is certainly the most complicated and involved one carried out under the current grant and represents significant progress in this area of intermediate energy nuclear physics. We incorporated nuclear medium effects into the scattering process fully consistent with the strictures of the Spectator Expansion of multiple scattering theory.

One of the most striking results is the prediction of the spin-observables A_y and Q for elastic proton scattering from light (^{16}O) as well as heavy (^{90}Zr, ^{208}Pb) nuclei at energies as low as 65 MeV. Another noteworthy result is the prediction of total cross section measurements for neutron scattering from light (^{12}C, ^{16}O) as well as heavy (^{90}Zr, ^{208}Pb) nuclei in the energy regime between $\sim$75 to 600 MeV. Our calculations show that a multiple scattering theory formulated in a sound way and applied in rigorous calculations is able to predict nucleon-nucleus elastic scattering observables accurately.

Very recently the PI and collaborators finished a comprehensive manuscript, outlining the theoretical framework of the Spectator Expansion and showing a selection of results for proton and neutron elastic scattering in the energy regime between ~65 and 400 MeV [1]. In this manuscript we concentrated mainly on results at lower energies, since there the corrections of the propagator due to the nuclear medium are most important. While implementing, testing and completing the calculations for different nuclei at many energies, we published several manuscripts concentrating on different physics aspects of elastic scattering of nucleons from nuclei [2, 3, 4]. In the following a summary of this work is presented.

The theoretical basis of our work is the Spectator Expansion of multiple scattering theory [5, 6, 7]. This expansion is based upon the idea that interactions between the projectile and the individual target nucleons inside the nucleus play the dominant role. In the Spectator Expansion the first order term involves interactions between the projectile and one of the target nucleons, the second order term involves the projectile interacting with two target nucleons and so forth. The many-body nature of the unperturbed propagator for the the projectile + target system makes it necessary to include a theoretical treatment of the many-body propagator as affected by the residual target nucleus.

At the heart of the standard approach to the elastic scattering of a single projectile from a target of A particles is the separation into two parts of the Lippmann-Schwinger equation for the the transition operator T, as given by

$$T = V + VG_0(E)T. \tag{1}$$

These two parts are an integral equation for T,

$$T = U + UG_0(E)PT, \tag{2}$$

where here U is the optical potential operator, and an integral equation for U

$$U = V + VG_0(E)QU. \tag{3}$$

In the above equations the operator V represents the external interaction ($V = \sum_{i=1}^{A} v_{0i}$), such that the Hamiltonian for the entire $A+1$ particle system is given by $H = H_0 + V$. Asymptotically the system is in an eigenstate of H_0, and the free propagator $G_0(E)$ for the projectile + target nucleus system is

$$G_0(E) = (E - H_0 + i\varepsilon)^{-1}. \tag{4}$$

where $H_0 = h_0 + H_A$, with h_0 being the kinetic energy operator for the projectile and H_A representing the target Hamiltonian. The projector Q is defined by $P + Q = 1$, with

$P = |\Phi_A\rangle\langle\Phi_A|/\langle\Phi_A|\Phi_A\rangle$ being the projector onto the ground state $|\Phi_A\rangle$ of the target, satisfying $[G_0, P] = 0$ and $H_A|\Phi_A\rangle = E_A|\Phi_A\rangle$.

With these definitions the transition operator for elastic scattering may be defined as $T_{el} = PTP$, in which case Eq. (2) can be written as

$$T_{el} = PUP + PUPG_0(E)T_{el}. \tag{5}$$

Thus, the transition operator for elastic scattering is given by a straightforward one-body integral equation, which requires, of course, the knowledge of the operator PUP. The theoretical treatment which follows consists of a formulation of the many-body equation, Eq. (3), where expressions for U are derived such that PUP can be calculated accurately without our having to solve the complete many-body problem.

With the assumption of purely two-body forces the operator U for the optical potential can be expressed as

$$U = \sum_{i=1}^{A} U_i \tag{6}$$

where U_i is given by

$$U_i = v_{0i} + v_{0i}G_0(E)Q\sum_{j=1}^{A} U_j. \tag{7}$$

The two-body potential, v_{0i}, acts between the projectile and the ith target nucleon. Through the introduction of an operator τ_i which satisfies

$$\tau_i = v_{0i} + v_{0i}G_0(E)Q\tau_i, \tag{8}$$

Eq. (7) can be rearranged as

$$U_i = \tau_i + \tau_i G_0(E)Q\sum_{j\neq i} U_j. \tag{9}$$

This rearrangement process can be continued for all A target particles, so that the operator for the optical potential can be expanded in a series of A terms of the form

$$U = \sum_{i=1}^{A} \tau_i + \sum_{i,j\neq i}^{A} \tau_{ij} + \sum_{i,j\neq i,k\neq i,j}^{A} \tau_{ijk} + \cdots. \tag{10}$$

This is the Spectator Expansion, where each term is treated in turn. The separation of the interactions according to the number of interacting nucleons has a certain latitude, due to the many-body nature of $G_0(E)$.

The first order term in the Spectator Expansion, τ_i is given by Eq. (8). Since for elastic scattering only $P\tau_iP$, or equivalently $\langle\Phi_A|\tau_i|\Phi_A\rangle$ need be considered, Eq. (8) can be reexpressed as

$$\begin{aligned}\tau_i &= v_{0i} + v_{0i}G_0(E)\tau_i - v_{0i}G_0(E)P\tau_i \\ &= \hat{\tau}_i - \hat{\tau}_i G_0(E)P\tau_i,\end{aligned} \tag{11}$$

where $\hat{\tau}_i$ is defined as the solution of

$$\hat{\tau}_i = v_{0i} + v_{0i}G_0(E)\hat{\tau}_i. \tag{12}$$

The combination of Eqs. (11) and (2) corresponds to the first order Watson scattering expansion [8]. If the projectile – target nucleon interaction is assumed to be the same for all target nucleons and if isospin effects are neglected then the KMT scattering integral equation [9] can be derived from the first order Watson scattering expansion.

The free propagator $G_0(E)$ may be written as

$$\begin{aligned}G_0(E) &= (E - h_0 - H_A + i\varepsilon)^{-1} \\ &= (E - h_0 - h_i - W_i - H^i + i\varepsilon)^{-1}\end{aligned} \tag{13}$$

with

$$W_i = \sum_{j\neq i} V_{ij} \tag{14}$$

and

$$H^i = H_A - h_i - W_i. \tag{15}$$

Since H^i has no explicit dependence on the ith particle, then Eq. (12) may be simplified by the replacement of H^i by an average energy E^i, so that Eq. (12) reduces to

$$\tilde{\tau}_i = v_{0i} + v_{0i}G_i(E)\tilde{\tau}_i. \tag{16}$$

Eq. (16) can also be reexpressed as

$$\tilde{\tau}_i = t_{0i} + t_{0i}g_iW_iG_i(E)\tilde{\tau}_i, \tag{17}$$

where the operators t_{0i} and g_i are defined to be

$$t_{0i} = v_{0i} + v_{0i}g_it_{0i} \tag{18}$$

and

$$g_i = [(E - E^i) - h_0 - h_i + i\varepsilon]^{-1}. \tag{19}$$

The quantity W_i represents the coupling of the struck target nucleon to the residual nucleus. The kinetic energy of the projectile is given by h_0 and the one of target particle i by h_i. (For more details see Ref. [1].)

In the explicit treatment of the propagator $G_i(E)$ it is necessary to consider specific forms of the potential W_i. So far, we have treated W_i as one-body operator, such as a shell-model or mean field potential. We took the attitude that this potential is already known and is extracted from single particle mean field potentials as calculated in various studies of nuclear structure. Now Eq. (17) can be written as

$$\tilde{\tau}_i = t_{0i} + t_{0i} g_i \mathcal{T}_i g_i \tilde{\tau}_i, \tag{20}$$

with $\mathcal{T}_i$ being given as the solution of a Lippmann-Schwinger type equation with the potential W_i as the driving term

$$\mathcal{T}_i = W_i + W_i g_i \mathcal{T}_i. \tag{21}$$

In the case that W_i is itself taken to be a one-body potential Eq. (21) becomes a one-body integral equation, which is easily solved numerically. This is the approach taken in all our calculations [1, 2, 3, 4]. While Eqs. (20) and (21) are completely equivalent to Eq. (17), a justification for the substitution of a Hartree-Fock or any other single particle mean field potential taken from a nuclear structure calculation is not strictly within the theoretical prerequisites of the Spectator Expansion, which demands that all of the two-body interactions be consistently represented by v_{0i}. Standard mean field or shell model calculations use an effective NN interaction for the reason that present microscopic nuclear structure calculations are unable simultaneously to use realistic free NN potentials and predict the experimental results. Hence it is not physically unreasonable to substitute a mean field potential for $W_i = \sum_{i,j\neq i} \tau_{ij}$, but this choice is *defacto* outside the strict demands of the Spectator Expansion.

The operator $\mathcal{T}_i$, representing the scattering of the struck target particle i from the residual nucleus, is calculated through the use of a one-body potential W_i. Nonlocal, spin-dependent potentials derived from realistic nuclear mean field models are used to represent the potential W_i given in Eq. (21). Two different mean field potentials are used in these calculations in order to give some hint about any model dependence which may exist. One is the nonrelativistic, non-local mean field potential taken from a Hartree-Fock-Bogolyubov microscopic nuclear structure calculation, which utilizes the density-dependent finite-ranged *Gogny D1S* nucleon-nucleon interaction [10, 11]. This model has been shown to provide accurate descriptions of a variety of nuclear structure effects. The second choice involves a nonrelativistic, local reduction of the mean field potential resulting from a Dirac-Hartree calculation based upon the $\sigma-\omega$ model [12]. The choice of these two potentials was mainly motivated through availability. A step by step description of the implementation of the nuclear mean field potential, consistent with the framework of the Spectator Expansion is given in Ref. [2].

The nucleon-nucleon (NN) t-matrix is another crucial ingredient in these calculations. For convenience our calculations use the full Bonn potential[13] and its extension above pion-production threshold [14] as input. Comparisons of different NN interactions in this context are planned for the future. It should be clearly understood that even if the underlying models for the NN interaction accurately describe the 'on-shell' NN data, there may still exist significant 'off-shell' differences between the various models, which could affect the predictions of the elastic nucleon-nucleus observables.

The first order folded effective NN t-matrix is then constructed with the operator, $\tilde{\tau}_i$, from Eq. (20):

$$\langle \tilde{\tau}_{eff} \rangle = \langle \vec{k}_0' \Phi_A | \sum_i \tilde{\tau}_i | \vec{k}_0 \Phi_A \rangle \ . \qquad (22)$$

These calculations are performed in momentum space and include spin degrees of freedom. We then evaluate the first order optical potential by solving Eq. (11) in the folded form. In the present calculations, which are performed in momentum space, $\langle \tilde{\tau}_{eff} \rangle$ enters in the 'optimum $\langle \tilde{\tau}_{eff} \rangle$ enters in the 'optimum factorized' or 'off-shell $\tau\rho$' form [15, 16] as

$$\langle \tilde{\tau}_{eff} \rangle \approx \tilde{\tau}(q, \mathcal{K}; E)\rho(q) \ , \qquad (23)$$

where $\vec{q} = \vec{k}_0' - \vec{k}_0$ and $\vec{\mathcal{K}} = \frac{1}{2}\left(\vec{k}_0' + \vec{k}_0\right)$; $\vec{k}_0'$ and $\vec{k}_0$ are the final and initial momenta of the projectile. This corresponds to a steepest descent evaluation of the 'full-folding' integral, in which the non-local operator $\tilde{\tau}$ is convoluted with the density $\rho(q)$ as indicated schematically in Eq. (22). For harmonic oscillator model densities it has been shown that the optimum factorized form represents the nonlocal character of U_{opt} qualitatively in the intermediate energy regime [17, 18]. Complete 'full-folding' calculations with more realistic nuclear densities are in progress. For the proton-nucleus scattering calculations the Coulomb interaction between the projectile and the target is included using the exact momentum space formalism described in Ref. [19]. A further remark is that an approximate treatment of the three-body kinematics involving the scattering of the struck target nucleon from the residual nucleus is used. This treatment is discussed at length in Ref. [2], and the approximation will eventually be eliminated from our calculations.

In this report only a few calculations are displayed, which are representative for the results we obtained through including the modification of the propagator due to the presence of the nuclear medium in a fashion consistent with the strictures of the Spectator Expansion. In a recent paper [4] we presented proton as well as nuclear scattering observables at 65 MeV projectile energy for ^{12}C, ^{16}O, ^{28}Si, ^{40}Ca, ^{56}Fe, ^{90}Zr and ^{208}Pb. In Fig. 1 a selection of those observables are shown, namely for ^{28}Si, ^{56}Fe, ^{90}Zr and ^{208}Pb. These calculations were performed at an energy which had been considered to be below the regime of applicability of the first order spectator expansion. However, there is a wealth of experimental data at this low energy for the above mentioned nuclei. It is very clear that the inclusion of the coupling of the struck target nuclear to the residual nucleus (solid line) considerably improves the description of the data compared to a non-local 'impulse approximation' calculation (dashed line). This is especially true for the description of the spin rotation parameter Q, in that the correction to the propagator causes the diffraction minima in the predictions of the differential cross sections to move to slightly higher angles and be closer to the data. This effect occurs for all nuclei under consideration, but is especially pronounced for heavy nuclei (^{90}Zr, ^{208}Pb), indicating a correct prediction of the effective size of the nuclei. Furthermore, the overall size of $d\sigma/d\Omega$ is predicted correctly over about five orders of magnitude (especially for ^{90}Zr). Fig. 2 shows the elastic scattering observables for ^{40}Ca and ^{90}Zr at 80 MeV projectile energy and for ^{16}O and ^{28}Si at 180 MeV. Again, the inclusion of the coupling of the struck target nucleon to the residual nucleus improves the description of the data considerably at the lower energy. At higher energies (180MeV) this effect decreases in magnitude.

In nuclear structure calculations the binding energy of the system in its ground state together with energies of certain low lying excited slates are the experimental information which must be closely reproduced to establish the reliability of the model wave functions and the various physical matrix elements implied thereby. In the present calculations of elastic nucleon-nucleus scattering the neutron total cross section, as function of scattering energy, could serve as a similar figure of merit. In Fig. 3 total neutron cross section data for ^{12}C, ^{16}O, ^{28}Si, ^{40}Ca, ^{90}Zr and ^{208}Pb are shown along with various calculations of σ_{tot}(E) at a number of energies. Because the data are so extensive, the 'usual' procedure has been reversed and the data are represented by dotted curves. The 'jitter' in these curves may be taken as indicative of the experimental uncertainty. The discrete points correspond to the calculated results. The solid diamonds include the modification of the free propagator through the Hartree-Fock-Bogolyubov mean field [10], except for ^{208}Pb, where W_i is taken from the Dirac-Hartree mean field [12], since HFB results are not available for ^{208}Pb at present. In each case the predictions are accord with the data from $\geq$ 65 MeV for the light nuclei and $\geq$100 MeV for the heavy nuclei. That is the theoretical predictions do extremely well in predicting the energy dependence of the total neutron cross section beyond the point where the data exhibit in pronounced structure. Fig. 3 is taken from Ref. [1]. We also published a separate detailed discussion on the neutron total cross sections for ^{16}O and ^{40}Ca [3].

As an indication as to how much has been gained by eliminating necessary earlier approximations to the full first order Spectator Expansion, point (represented as crosses) are shown at 100 and 200 MeV for ^{16}O, ^{40}Ca, ^{90}Zr and ^{208}Pb, which were calculated using the so-called 'local free $t\rho$' approximation. This consists of multiplying the on-shell NN scattering amplitude $t(q)$ with the one-nucleon density $\rho(q)$ for the target nucleus. These 'local free $t\rho$' results are significantly larger than the experimental values, in some cases, especially for the heavier elements, this discrepancy can be as large 25-30%. This gross failure of the local approximation casts doubt upon some of its early successes, and certainly creates serious reservation about many attempts to account for the failures of the local approximation by introduction of new effects, which are not cleanly consistent with a many body scattering theory. The points represented by the stars represent calculations performed with the free propagator G_0(E) of Eq. (12), where the target Hamiltonian is represented by a c-number. Those points contain the complete off-shell structure of the NN t-matrix in the optimum factorized form, but the coupling of the struck target nucleon to the residual nucleus is omitted. As Fig. 3 shows, this effect grows as the nuclei become heavier. In addition it is most prevalent in the regime between 100 and 200 MeV projectile energy and becomes almost negligible at higher energies.

In summary, we developed and implemented a theoretical framework, consistent with strictures of the Spectator Expansion of multiple scattering theory, to include the coupling of the struck target nucleon to the residual nucleus. The basic inputs to our calculations are the free fully off-shell NN interaction and realistic nuclear single particle densities. There are **no** adjustable parameters in the calculations. We found, that as the calculations include more complex degrees of freedom within a well-defined theoretical framework, the predictions invariably provide an improved description of the data.

Our work extended the viability of microscopic calculations of elastic scattering of protons and neutrons from nuclei to energies as low as $\sim$65 MeV projectile energy, and we obtain an overall good description of elastic proton and neutron scattering observables. To our knowledge these are presently the most extensive systematic microscopic calculations in the energy regime between $\sim$65 to 400 MeV projectile energy.

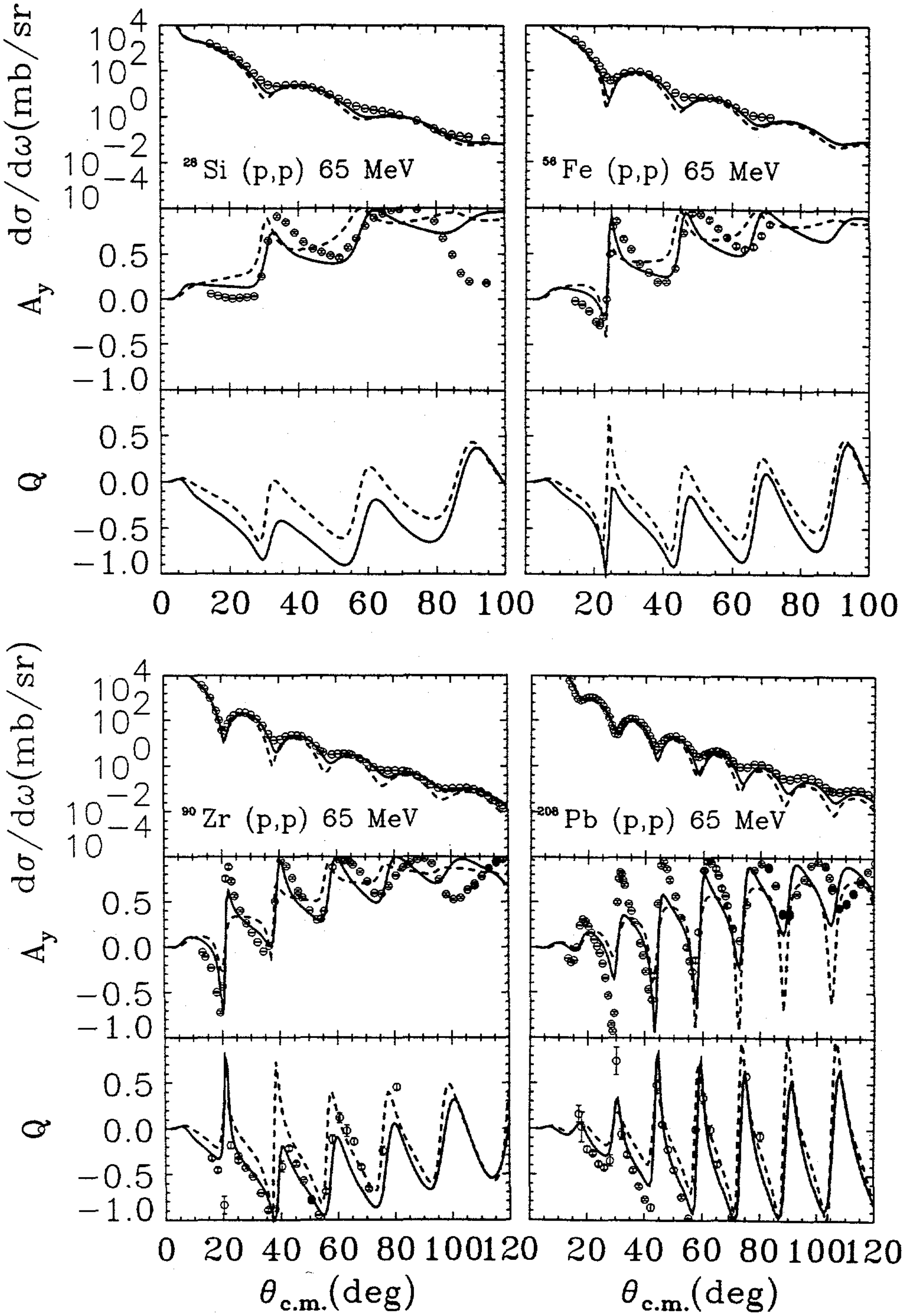

Fig. 1: The angular distribution of the differential cross-section ($\frac{d\sigma}{d\Omega}$), analyzing power (A_y) and spin rotation function (Q) are shown for elastic proton scattering from ^{28}Si, ^{56}Fe, ^{90}Zr and ^{208}Pb at 65 MeV laboratory energy. All calculations are performed with a first-order optical potential obtained from the full Bonn interaction [13] in the optimum factorized form. The solid curves include the modification of the propagator due to the HFB mean field [10], except for ^{208}Pb which is based on the DH mean field [12] (solid lines). The free, non-local impulse approximation is given by the dashed curves. The data are taken from Ref. [20].

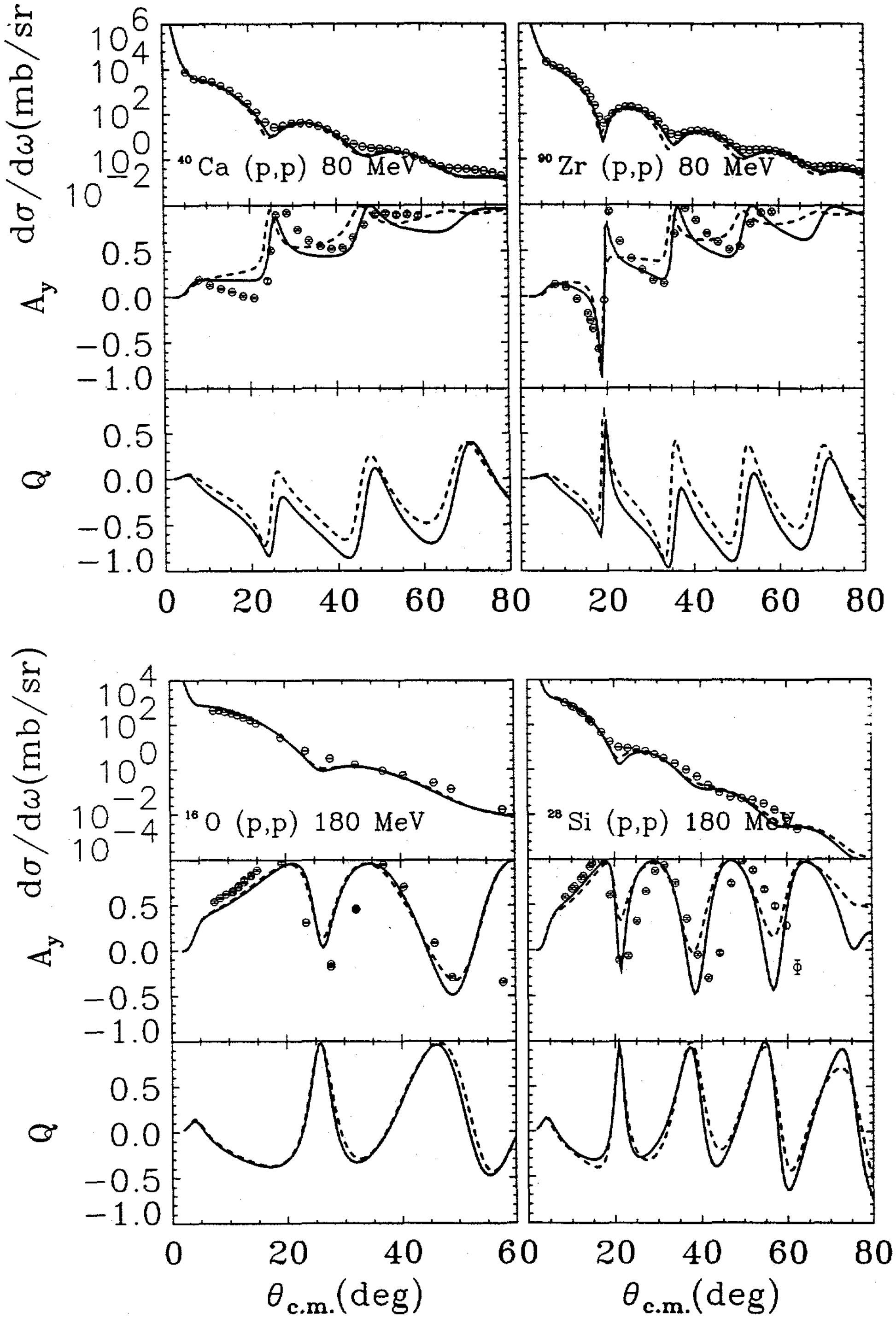

Fig. 2: Same as Fig. 1 for elastic proton scattering from ^{40}Ca and ^{90}Zr at 80 MeV and ^{16}O and ^{28}Si at 180 MeV laboratory energy. All calculations are performed with a first-order optical potential obtained from the full Bonn interaction [13] in the optimum factorized form. The solid curves include the modification of the propagator due to the HFB mean field [10] (solid lines). The free, non-local impulse approximation is given by the dashed curves. The data for ^{40}Ca at 80 MeV are from Ref. [21], for ^{90}Zr at 80 MeV from Ref. [22], for ^{16}O at 180 MeV from Ref. [23] and for ^{28}Si at 180 MeV from Ref. [22].

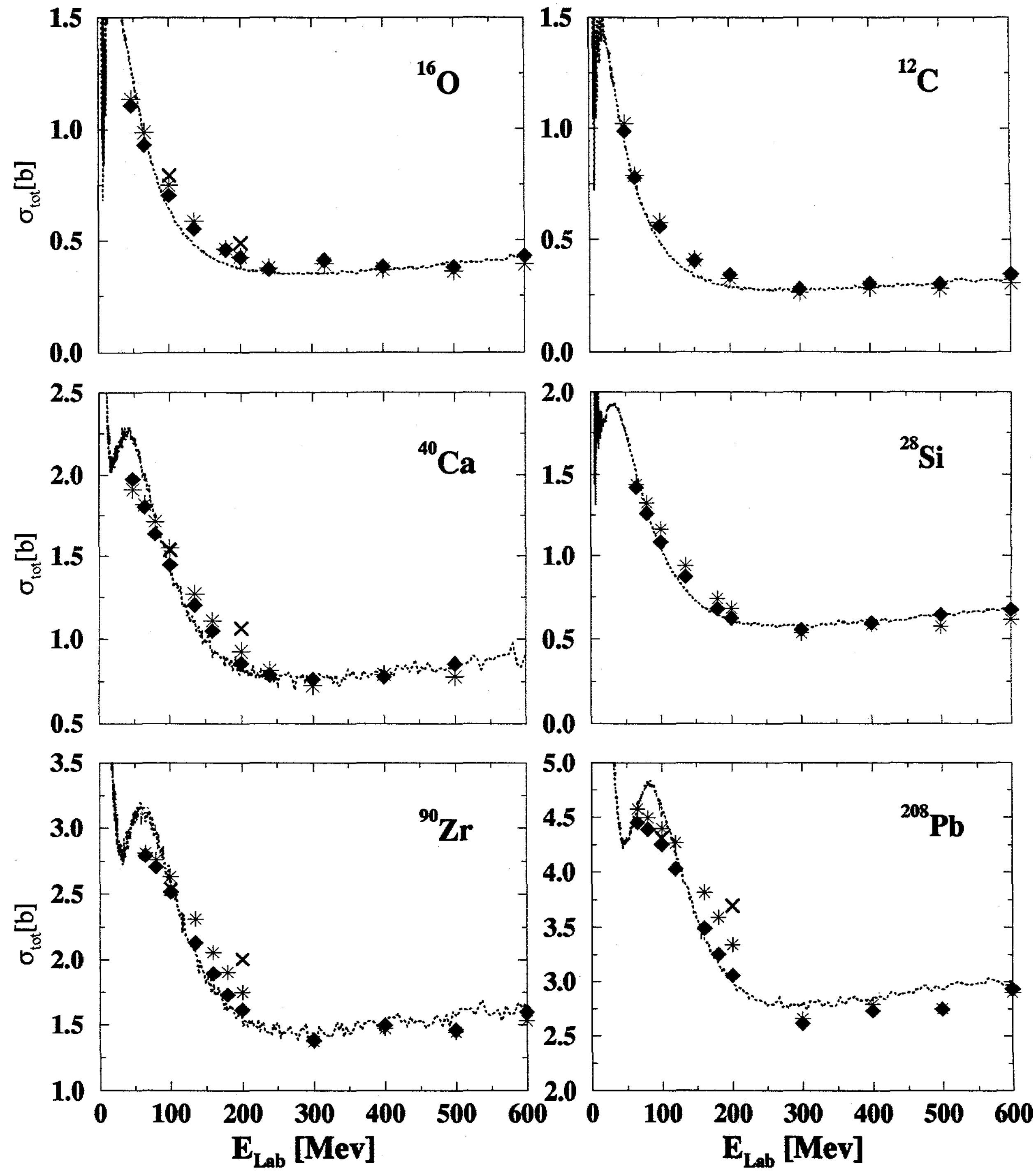

Fig. 3: The neutron-nucleus total cross-sections for scattering from ^{12}C, ^{16}O, ^{28}Si, ^{40}Ca, ^{90}Zr, and ^{208}Pb are shown as a function of the incident neutron kinetic energy. The dotted line represents the data taken from Ref. [24, 25]. The solid diamonds correspond to the calculations including the propagator modification due to the HFB mean field [10] (in case of ^{208}Pb of the DH mean field [12]). The star symbols indicate the 'free' calculations using the full Bonn free NN t-matrix [13] only. The cross symbols represent a local 'on-shell $t\rho$' calculation, which uses only the on-shell values of the same t-matrix.

(b) Relation to Ongoing and Planned Neutron Scattering Experiments.

Quite recently measurements of 65 MeV neutron-nucleus elastic differential cross sections were published [26]. The PI and collaborators immediately took this opportunity to study neutron as well as proton elastic scattering at this energy [4]. A comparison at this energy is particularly fruitful, since an abundance of proton elastic scattering data also exists. As example from Ref. [4] the differential cross section for neutron and proton scattering from ^{208}Pb at 65 MeV is shown in Fig. 4. The very good representation of the data by our calculations was somewhat unexpected. They clearly showed the importance of the coupling of the struck target nucleon to the residual nucleus. One might presumed that at this low an energy higher order terms in the spectator expansion become important. The data suggest that these terms may not be strongly structured and so will, perhaps, raise the forward cross section and fill in the sharp diffraction minima. A change in the spin structure due to higher order terms may only be apparent at large scattering angles. Further work is required before a clear understanding of the reasons for the success of the first order calculations at this low energy can be completely be understood.

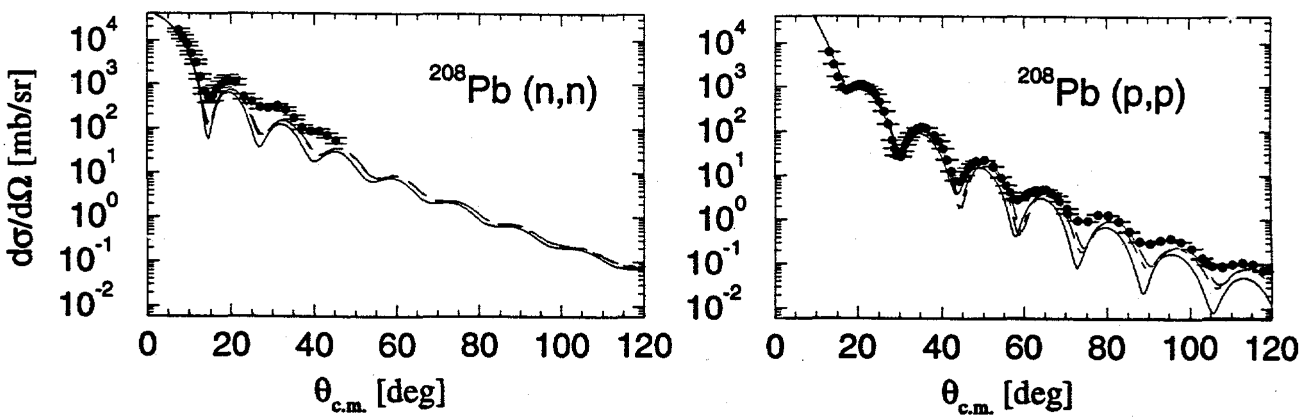

Fig. 4: The angular distribution of the differential cross-section ($\frac{d\sigma}{d\Omega}$) for elastic neutron and proton scattering from ^{208}Pb at 65 MeV laboratory energy. The neutron data are from Ref. [26], while the proton data are from Ref. [20]. The solid lines correspond to a calculation of the first order optical potential based on the free NN t-matrix from the full Bonn model [13] as input. The dashed and dash-dotted lines include the propagator modification due to the nuclear mean field. For the dash-dotted curve a Hartree-Fock-Bogolyubov [10] is used, for the dashed curve a Dirac-Hartree mean field [12].

It is obvious from Fig. 4 that the theoretical curve for the neutron elastic differential cross section falls below the data in forward angles, while the prediction for the proton elastic differential cross section describes the data almost perfectly throughout the first three diffraction minima. The reason may be that in the proton case the Coulomb effect dominates at small scattering angles and thus masks any underprediction. It may also be argued that the neutron projectile should be able to penetrate further into the nucleus than a proton projectile, due to the lack of the coulomb barrier. This may perhaps mean that for heavier nuclei, neutron scattering might be more sensitive to higher order multiple scattering effects as well as to the propagator corrections we employ. This may illustrate the enhanced value and impact of having combined neutron and proton data sets.

Currently neutron elastic differential cross section measurements at energies between 60 and 260 MeV for ^{40}Ca, taken at the WNR facility at LAMF, are being analyzed by the UC-Davis group [27]. The PI and collaborators already provided theoretical predictions at 160 MeV neutron energy and it was found that they agree very well with the preliminary analysis [27]. At The Svedberg Laboratory, Uppsala, measurements of neutron elastic cross sections for ^{208}Pb, ^{40}Ca and ^{16}O are proposed at 46 and 100 MeV [28]. The PI and collaborators are in contact with this group and will provide theoretical contributions. These measurements are very timely for providing deeper insight into the mechanisms of multiple scattering expansions.

(c) Isospin Effects in Elastic Proton-Nucleus Scattering.

Very early in the grant period we investigated isovector degrees of freedom in proton-nucleus elastic scattering [29]. Isovector effects, i.e. mechanisms which distinguish neutron from proton scattering, can be explicitly treated without any difficulty in the first-order Spectator Expansion. The τ_i's in Eq. (11) are expressed separately for each i, thus no assumption about the isospin character of the NN interaction is made at this stage. The proton-proton and proton-neutron interactions are treated independently in Eq. (11). Therefore the subsequent optical potential is the sum of two different contributions

$$\begin{aligned} U &= \sum_{i=1}^{Z} \tau_{p,i} + \sum_{i=1}^{N} \tau_{n,i} \\ &= Z\tau_p + N\tau_n. \end{aligned} \tag{24}$$

As is obvious from Eq. (24), the isovector character of τ_p and τ_n as well as their corresponding convolution with the proton and neutron distributions is taken into account in a completely consistent fashion. We applied this formulation in all our subsequent calculations, especially in those described under (a). From this point of view, isovector effects are taken into account correctly in all our calculations.

In this earlier publication [29] we compared our formulation with calculations based on the KMT formalism [9], where isovector effects are usually averaged out, since their inclusion is quite tedious. We tested the accuracy of the KMT averaging procedure for proton incident energies from 200 MeV to 800 MeV and found that it is very good for nuclei larger than ^{4}He. We then used our formalism to look at the impact of differences in the neutron density on elastic proton scattering observables. Although the proton density distribution is very well determined from electron scattering data, this is certainly not the case for the neutron distribution.

We found that for a traditionally studied $N \neq Z$ nucleus like ^{208}Pb the isovector effects are quite small in the energy regime above 200 MeV projectile energy and in this regime it may remain unrealistic to expect to be able to extract detailed quantitative information about the target nucleus from proton-nucleus elastic reactions. However, the situation may be different at the lower energies where the explicit formulation of the structure of the target nucleus enters. For nuclei with a much larger neutron excess, like the 'halo' nuclei, this effect may even be quite large. We plan to study halo nuclei in the near future.

(d) Ongoing Work: Full-Folding Calculations of the first-order Optical Potential

The next major step in bringing all first order effects into nucleon-nucleus scattering in a consistent fashion with the Spectator Expansion is the calculation of a 'full-folding' optical potential using the same realistic nuclear wave functions that give rise to the medium modifications. In an earlier publication by the PI and collaborators [17], a full-folding calculation had been carried out for ^{16}O with simplistic harmonic oscillator wave functions. This simple model calculation indicated that a convolution of the fully off-shell NN t-matrix with the nuclear density matrix improves the description of elastic p-nucleus observables in the energy regime between 200 and 500 MeV projectile energy. It showed deficiencies at lower energies, indicating that there the modification of the nuclear medium has to be taken into account.

The model calculation of Ref. [17] could be carried out relatively easily, since all angle integrations could be performed analytically and energy shifts in the NN t-matrix due to frame transformations were neglected. According to our present standards of calculation, those approximations are no longer tolerable. For realistic nuclear wave functions all integrations have to be carried out numerically in three dimensions. We are developing a generalized 'full-folding' scheme based on a Monte Carlo integration using Quasi Random Numbers [30] together with importance sampling for the different integration variables. We developed the different numerical ingredients for a full-folding calculation of the optical potential for scattering from ^{16}O. We chose this nucleus as our first general case in order to have a comparison with the much simpler calculation of Ref. [17]. We are setting up the calculations in such a way that they can take advantage of the massively parallel computers Cray T3D at the Ohio Supercomputer Center and the Intel Paragon at Oak Ridge National Laboratory. In order to have a clear picture on the energy dependence of the NN t-matrix as well as its three-dimensional form as function of momenta, we animated the NN t-matrix as function of energy and as function of the angle between the two vector momenta. We found the use of visualization tools very useful in judging how to set up our calculations. At present we are performing the numerical tests on the different parts of the calculation. Eventually, of course we aim for 'full-folding' calculations for light as well as heavy nuclei.

3. Few-Body Systems described by Effective Hadronic Field Theories.

In the area of Few-Body physics the PI was involved in two different projects. One was a study of neutron-proton (np) scattering at backward angles and was carried out in collaboration with an experimental group at Ohio University. The study was presented at the XIV International Conference on Few-Body Physics, 1994 in Williamsburg. The second project was a study of the sensitivity of the nucleon-nucleon (NN) tensor force to explicit pionic degrees of freedom, and was presented at the DNP meeting 1994 in Williamsburg. The following subsections describe in some detail the work carried out under the current grant from the U.S. Department of Energy.

(a) The Neutron-Proton Differential Cross Section at Backward Angels

The H(n,p) differential cross section at backward c.m. angles can be viewed as the simplest elemental charge exchange reaction and should display a similar characteristic as the nuclear charge exchange differential cross section. Recent measurements of the np differential cross section ($d\sigma/d\Omega$) at backward angles [32, 33] show a systematic deviation from previously obtained data. In the energy regime between 60 to 200 MeV the recent values for $d\sigma/d\Omega$ at angles close to $\theta_{cm} = 180^o$ are roughly 10% larger (Fig. 5).

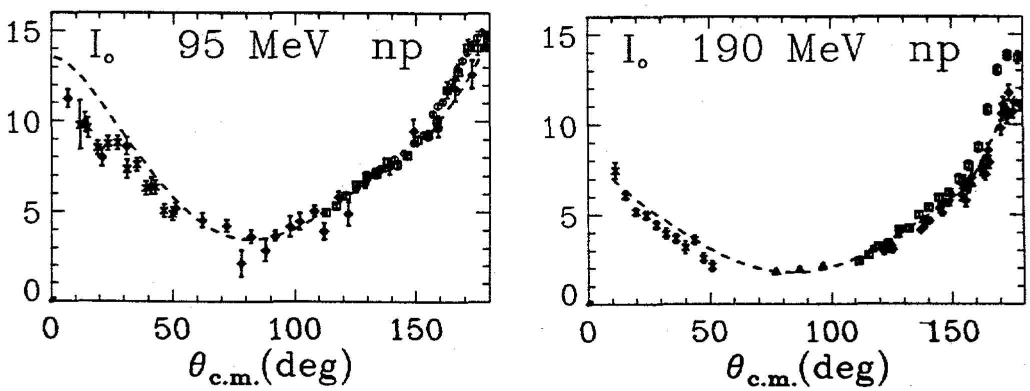

Fig. 5: The np differential cross section at 95 and 190 MeV as function of the scattering angle in the laboratory system. The data at 95 MeV are taken from Ref. [32] (∘), Ref. [33] (□), Ref. [36] (⋄) and Ref. [37] (×). The data at 190 MeV are from Ref. [33] (□), Ref. [37] (×), Ref. [38] (△) and Ref. [39] (⋄). The dashed line represents the Arndt analysis VZ40 (1992).

In view of these experimental discrepancies and the recent discussion about the size of the pion-nucleon coupling [34], it was compelling to investigate to what extent the np differential cross section at backward angles is determined by the long range Yukawa part of the one-pion potential, and if this observable places any constraints on the long range part of the NN interaction.

We studied the sensitivity of $d\sigma/d\Omega$ at back angles to the size of $g_\pi^2/4\pi$ within the framework of one-boson-exchange (OBE) models [36] and the full Bonn NN interaction [13]. We preferred this approach, since applying meson exchange models allows an explicit change of meson couplings and the investigation of the effects of those changes in all partial waves. Our studies showed that, independent of the applied model, the size of $d\sigma/d\Omega$ at 180^o varies almost linearly with the size of $g_\pi^2/4\pi$, provided σ_{tot} is kept at a fixed value by readjusting the central attraction and all other couplings remain fixed.

In order to obtain a more detailed understanding we decomposed $d\sigma/d\Omega$ into its angular momentum states with even l contribute to $d\sigma/d\Omega$ symmetrically around $\theta_{cm} = 90^o$, states with odd l antisymmetrically. Due to the properties of the Legendre polynomials, the one-pion-exchange contributions add up coherently for $\theta_{cm} = 180^o$. Fig. 6 shows that the size of $d\sigma/d\Omega$ at backward angles is dominated by D-waves (in particular $^3D_2$) as well as by higher partial waves. Both, the high partial waves as well as $^3D_2$ are dominated by pion-exchange contributions and their magnitude varies with the size of $g_\pi^2/4\pi$. This feature was charateristic for all OBE models we studied, as well as for more complicated multi-meson exchange models.

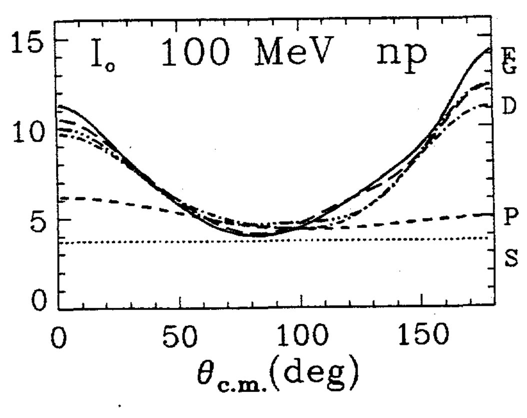

Fig. 6 Successive contributions of partial waves to the np differential cross section at 100 MeV. The solid line represents the calculation with $g_\pi^2/4\pi$=14.2 using partial wave contributions up to J=12. Explicit partial wave contributions are shown for S(dot), S+P(dash), S+P+D(dash-dot), S+P+D+F(dash-3dots), S+P+D+F+G(long dash).

We also found, that although the high partial waves do not display any cutoff dependence, they vary with the type of three-dimensional reduction used to cast the Bethe-Salpeter equation into Lippmann-Schwinger form. These reductions (e.g. Blankenbecler-Sugar) typically introduce factors E/M (M representing the nucleon mass, $E = \sqrt{M^2 + k^2}$), which can be viewed as energy dependent 'renormalization' of the coupling constant. While at the deuteron pole, these factors are irrelevant, at energies larger than 100 MeV their presence reduces higher partial waves about 5%.

We also investigated a possible sensitivity to the ρ-vector and tenor coupling, and found that a strong ρ-tensor coupling (characterized by $\kappa = f_\rho/g_\rho$) is needed in order to obtain a quantitative description of the NN phase shifts. Variations of about 1-% around $\kappa = 6.1$, which is well within the experimental uncertainties of this parameter, has little effect on the back angle differential cross section. An explicit calculation of the correlated $\pi\pi$-exchange, conventionally represented by the exchange of a σ ($J^p=0^+$) and ρ ($J^p=1^-$) meson, shows that the $\pi\pi$-exchange in the $J^p=0^+$ channel is longer ranged than the exchange of a 'σ-meson' and contributes to F- and G-waves [40]. Our estimates indicate that the correlated $\pi\pi$-exchange can contribute to higher values of $d\sigma/d\Omega$ at backward as well as forward angles. Our preliminary conclusion is that the currently favored low value of $g_\pi^2/4\pi = 13.8$ is not able to describe the new data for the backward angle differential cross section within a 'traditional' meson exchange model. Additional effects, like the explicit treatment of the $\pi\pi$-exchange may have to be taken into account if the lower pion coupling is to be favored.

A new precise measurement of the H(n,p) differential scattering cross section in the energy range of 50 - 250 MeV at WNR at LAMF was made in summer 1994 by the Principal Investigator B.K. Park, J.L. Ullman and J. Rapaport [41, 33]. The analysis of the data is presently being carried out. The PI will perform additional studies in connection with the final experimental results.

References

[1] C. R. Chinn, Ch. Elster, R. M. Thaler, and S. P. Weppner, submitted to Phys. Rev. C, and *http://xxx.lanl.gov*, preprint nucl-th/9503027.

[2] C.R. Chinn, Ch. Elster, and R.M. Thaler, Phys. Rev. **C48**, 2956 (1993).

[3] C.R. Chinn, Ch. Elster, R.M. Thaler, and S.P. Weppner, Phys. Rev. **C51**, 1033 (1995).

[4] C. R. Chinn, Ch. Elster, R. M. Thaler, and S. P. Weppner, Phys. Rev. **C51**, 1418 (1995).

[5] D.J. Ernst, J.T. Londergan, G.A. Miller, and R.M. Thaler, Phys. Rev. **C16**, 537 (1977).

[6] E. R. Siciliano and R. M. Thaler, Phys. Rev. **C16**, 1322 (1977).

[7] P.C. Tandy and R.M. Thaler, Phys. Rev. **C22**, 2321 (1980).

[8] K.M. Watson, Phys. Rev. **89**, 575 (1953); N.C. Francis and K. M. Watson, *ibid.* **92**, 291 (1953).

[9] A. Kerman, M. McManus, and R. M. Thaler, Ann. Phys. **8**, 551 (1959).

[10] See for example J.F. Berger, M. Girod, and D. Gogny, Nucl. Phys. **A502**, 85c (1989); J.P. Delaroche, M. Girod, J. Libert and I. Deloncle, Phys. Lett. **B232**, 145 (1989).

[11] J.F. Berger, M. Girod, and D. Gogny, Comput. Phys. Commun. **63**, 365 (1991).

[12] C.J. Horowitz and B.D. Serot, Nucl. Phys **A368**, 503 (1981).

[13] R. Machleidt, K. Holinde, and Ch. Elster, Phys. Rep. **149**, (1987).

[14] Ch. Elster and P.C. Tandy, Phys. Rev. **C40** (1989), 881; Ch. Elster, Ph.D. thesis, University of Bonn, 1986.

[15] D. J. Ernst and G. A. Miller, Phys. Rev. **C21**, 1472 (1980); D. L. Weiss and D. J. Ernst, Phys. Rev. **C26**, 605 (1982); D. J. Ernst, G. A. Miller and D. L. Weiss, Phys. Rev. **C27**, 2733 (1983).

[16] A. Picklesimer, P. C. Tandy, R. M. Thaler, and D. H. Wolfe, Phys. Rev. **C30**, 1861 (1984).

[17] T. Cheon, Ch. Elster, E. F. Redish, and P. C. Tandy, Phys. Rev. **C41** (1990), 841.

[18] R. Crespo, R. C. Johnson, and J. A. Tostevin, Phys. Rev. **C41** (1990), 2257.

[19] C.R. Chinn, Ch. Elster, and R.M. Thaler, Phys. Rev. **C44**, 1569 (1991).

[20] H. Sakaguchi, M. Nakamura, K. Hatanaka, A. Goto, T. Noro, F. Ohtani, H. Sakamoto, H. Ogawa, and S. Kobayashi, Phys. Rev. **C 26**, 944 (1982).

[21] A. Nadasen, P. Schwandt, P.P. Singh, W.W. Jacobs, A.D. Bocher, P.T. Debevec, M.D. Katchuck, J.T. Meek, Phys. Rev. **C23**, 1023 (1981).

[22] P. Schwandt, H.O. Mayer, W.W. Jacobs, A.D. Bacher, S.E. Vigdor, M.D. Kartchuck, Phys. Rev. **C26**, 55 (1982).

[23] J.Kelly *et al.* Phys. Rev. **C41** 2504 (1990).

[24] R. W. Finlay, W. P. Abfalterer, G. Fink, E. Montei, T Adami, P. W. Lisowski, G. L. Morgan and R. C. Haight, Phys. Rev. **C 47**, 237 (1993).

[25] R.W. Finlay, G. Fink, W. Abfalterer, P. Lisowski, G.L. Morgan, and R.C. Haight, in *Proceedings of the Internat. Conference on Nuclear Data for Science and Technology*, edited by S.M. Qaim (Springer-Verlag, Berlin, 1992), p. 702.

[26] E. L. Hjort, F. P. Brady, J. L. Romero, J. R. Drumond, D. S. Sorenson, J. H. Osborne and B. McEachern, Phys. Rev. **C50**, 275 (1994).

[27] Jack Osborne, private communication

[28] Jan Blomgren, *et al.*, Proposal to the TSL: Experimental Studies of Neutron Scattering.

[29] C.R. Chinn, Ch. Elster, and R.M. Thaler, Phys. Rev. **C47**, 2242 (1993).

[30] W.H. Press and S.A. Teukolsky, Comp. in Phys. (1989), 76.

[31] For a discussion see T.E.O. Ericson and W. Weise, 'Pions in Nuclei', Oxford University Press, 1988; and T.E.O. Ericson, Inv. Talk at the Int. Symp. on Spin-Isospin Responses and Weak Processes in Hadrons and Nuclei, Osaka, March 8-10, 1994.

[32] [2] T. Rõnnqvist *et al.*, Phys. Rev. **C45**, R496 (1991).

[33] J. Rapaport, private communication

[34] T.E.O. Ericson, Nucl. Phys. **A543**, 409c (1992); V.G.J. Stoks, R. Timmermans, and J.J. de Swart, Phys. Rev. **C47**, 512 (1993).

[35] R. Machleidt, Adv. in Nucl. Phys. **19**, 189 (1989).

[36] J.P. Scanlon, G.H. Stafford, J.J. Thresher, P.H. Bowen, and A. Langsford, Nucl. Phys. **41**, 401 (1963).

[37] A.J. Bersbach, R.E. Mischke, and T.J. Devlin, Phys. Rev. **D13**, 535 (1976).

[38] A.R. Thomas, P. Spalding, and E.H. Thorndike, Phys. Rev. **167**, 1240 (1964).

[39] B.E. Bonner *et al.* Phys. Rev. Lett. **41**, 1200 (1978).

[40] H.-C. Kim, J.W. Durso, and K. Holinde, Preprint KFA-IKP(TH)-1993-27.

[41] LANL Neutron Program Advisory Committee Report LA-UR-94-1891.

Students participating in Research Projects during the Grant Period:

S.P. Weppner
Ph.D. Thesis (ongoing)
Research Project: 'Generalized full-folding calculations of the first order optical potential for elastic nucleon-nucleus scattering within the Spectator Expansion.'

L. Wang
Masters Degree, Fall 1994
Research Project: 'Low Energy Behavior of Energy Dependent One-Boson-Exchange Nucleon-Nucleon Interactions.'

presently employed at Digital Concepts, Dayton, OH

B.E. Barmore
Bachelors Degree, Summer 1993
Undergraduate Thesis
presented to the Honors Tutorial College at Ohio University: 'Sensitivity of Back Angle (n,p) Scattering to the Pion-Nucleon Coupling Constant.'

presently Graduate Student
at the College of William and Mary, Williamsburg, VA.
Advisor: D. Walecka

E. Evans
Bachelors Degree, expected Summer 1995
Undergraduate Thesis Research Project (ongoing):
'Effect of a nonlocal Yukawa interaction on the bound state properties. of a two and three fermion bound state.'

Ohio University

Grant DE-FG02-93ER40756

For the Budget Period November 1, 1994 through October 31, 1995

1.	Total DOE Funds Obligated	$47,000
2.	Estimated Total Project Costs through the Current Budget Period chargeable to DOE	$47,000
3.	Anticipated DOE Funds Available for Carry Over into the next Budget Period	-0-